Environmental Technology & Innovation 32 (2023) 103405

Contents lists available at ScienceDirect

Environmental Technology & Innovation

journal homepage: www.elsevier.com/locate/eti

Accelerated aging of polyvinyl chloride microplastics by UV irradiation: Aging characteristics, filtrate analysis, and adsorption behavior

Kefu Wang [a], Kangkang Wang [a], Siqi Liang [a], Changyan Guo [a,*], Wei Wang [b,c,**], Jide Wang [a,*]

[a] Key Laboratory of Oil and Gas Fine Chemicals, Ministry of Education & Xinjiang Uygur Autonomous Region, School of Chemical Engineering and Technology, Xinjiang University, Urumqi, China
[b] Department of Chemistry, University of Bergen, Bergen 5007, Norway
[c] Center for Pharmacy, University of Bergen, Bergen 5020, Norway

ARTICLE INFO

Keywords:
Polyvinyl chloride microplastics
UV aging
Aging characteristics
Adsorption
Leaching analysis

ABSTRACT

The extensive use of plastic products by people has led to the prevalence of microplastics (MPs) in aquatic and terrestrial ecosystems. MPs will be able to undergo multiple aging processes and release dissolved organic matter (DOM) in the aquatic environment, thereby further affecting the ecosystem. Therefore, this thesis systematically investigated the photo-aging properties of polyvinyl chloride (PVC), and characterized the changes in physicochemical properties; in addition, the DOM composition and fluorescence characteristics of MPs leachate were characterized by using TOC and 3D-EEMs. Our results showed that the O/C ratio can quantitatively characterize the surface aging of MPs. Furthermore, We chose Malachite green (MG) and Sulfamethoxazole (SMX), which are abundantly present in the aqueous environment, as the target pollutants, through adsorption experiments we established the regression equations of the equilibrium adsorption capacity of aging MPs with O/C ratio or CI and mean particle size. Exploring the relationship between aging properties and the adsorption capacity of microplastics can help predict the degree of aging and accumulation of hydrophilic contaminants in the natural environment.

1. Introduction

Once in the environment, plastics lead to potentially severe consequences for aquatic environments and inestimable long-term implications for the world's ecosystems (Chae and An, 2018; de Souza Machado et al., 2018; Galloway et al., 2017). In particular, microplastics (MPs), defined as plastic fragments smaller than 5 mm (Frias and Nash, 2019; Law and Thompson, 2014), are environmental contaminants which aroused increasing scientific and public concern (Andrady, 2011; Alimi et al., 2018). Due to their high content, small particle size, large specific surface area, and long migration distances, MPs may be harmful to the environment and human health (Guo et al., 2020; Huang et al., 2021), and they are widely detected in the ocean (Mu et al., 2019), inland waters (Su

* Corresponding authors.
** Corresponding author at: Department of Chemistry, University of Bergen, Bergen 5007, Norway.
E-mail addresses: gcyslw@xju.edu.cn (C. Guo), wei.wang@uib.no (W. Wang), awangjd@sina.cn (J. Wang).

https://doi.org/10.1016/j.eti.2023.103405
Received 19 August 2023; Received in revised form 5 October 2023; Accepted 8 October 2023
Available online 12 October 2023

et al., 2016), soil (Lv et al., 2019), and the atmosphere (Chen et al., 2020). MPs have also been discovered in relatively unexplored regions, including Mount Everest (Napper et al., 2020), Marianas Trench (Peng et al., 2018) and polar regions (Peeken et al., 2018). In aquatic environments, MPs may adsorb typical contaminants such as heavy metals (Li et al., 2022), dyes (Anastopoulos et al., 2022), pesticides (Jiang et al., 2020), drugs (Hu et al., 2020) and antibiotics (Yu et al., 2020), And it is possible to transport them to organisms such as marine mammals (Zantis et al., 2021), cetaceans (Zhu et al., 2019), birds (Masiá et al., 2019), sea turtles (Duncan et al., 2019), zooplankton (Frias et al., 2014), fish (Neves et al., 2015), chickens (Huang et al., 2021) and even humans (Leslie et al., 2022), resulting in a dual toxic effect on organisms. Moreover, adverse effects upon ingestion have been demonstrated under laboratory conditions (Prokić et al., 2019). Therefore, further studies are needed to fully understand the role of MPs in contaminant transport.

Plastic waste products are widely distributed in the environment, exposed to UV irradiation and prone to thermal degradation, biodegradation, and oxidation reactions for a long time (Andrady, 2011; Jahnke et al., 2017; Wang et al., 2023a). MPs exposed to the natural environment have experienced a number of ageing processes due to a combination of continuous physicochemical factors. Different aging processes based on current literature; photochemical degradation is considered to be an important process of hydrocarbon polymers aging (Andrady, 2015; Gewert et al., 2015). The aging behavior of polymers under different environmental conditions has been extensively studied so far. A number of studies have reported the ageing of MPs under accelerated photodegradation conditions outdoors or in the laboratory (Gewert et al., 2015; Gardette et al., 2013; Singh and Sharma, 2008; Rivaton and Gardette, 1998), and they concluded that the morphological structure, elemental composition and molecular weight of MPs changed significantly, this process roughened their surfaces, formed porous surfaces, increased the specific surface area and oxygen-containing functional groups (Jiang et al., 2023), the production of these affect the polarity and hydrophobicity of MPs (Jiang et al., 2022), thus enhance the adsorption capacity (Hanun et al., 2021; Mao et al., 2020); at the molecular level, the chemical structure of MPs is influenced, such as chain breakage, particle size, and molecular weight distribution (Liu et al., 2021).

In addition, The most serious structural damage to plastic surfaces is caused by UV light irradiation, and this damage further supports the release of dissolved organics into the aqueous phase (Potthoff et al., 2017). Given that plastic-derived DOM may contain several additives and/or carbon-chain scission products, and that many of these substances are light-absorbing (Gewert et al., 2018; Suhrhoff and Scholz-Böttcher, 2016), it is necessary to explore the feasibility of detecting these plastic-derived substances by employing UV–visible and/or fluorescence spectroscopy. Romera-Castillo et al. (2018) have reported that plastic litter in the ocean releases ~23,600 tons of MPs-DOM per year, even accounting for 10% of DOM in the top 40-μm marine surface microlayer (Romera-Castillo et al., 2018). Therefore, further exploring the environmental chemical behavior of MP-DOM can help to understand the environmental impact associated with MPs. Quite a few published studies have documented the occurrence of plastic-derived DOM (Romera-Castillo et al., 2018; Galgani et al., 2018). Unfortunately, information on the aging behavior of MPs and the potential effect of aging on their adsorption of environmental pollutants is limited. therefore, it is necessary to investigate the relationship between the degree of aging of MPs and their adsorption capacity.

MPs in the environment can enrich contaminants from the surrounding environment and ingest into the body by organisms, thus altering their bioaccumulation (Wang et al., 2020a; Wardrop et al., 2016). Aging alters the interactions between MPs and contaminants (e.g., hydrophobic, π-π, electrostatic, and hydrogen bonding interactions), because aging causes changes in the surface properties of MPs such as reduced hydrophobicity, increased polarity and charge (Liu et al., 2020a; Sun et al., 2020). Thus, aged MPs may exhibit a different role in the bioaccumulation of contaminants than unaged ones. In general, the aging process appears to enhance the toxic effects of additives contained in MPs and cause fractures and chain breaks, which results in the release of more additives. Aging also causes polymer fracture and oxidation to release oligomers or oxidation products (e.g., phenols, acetophenones, and carboxylation products) (Gewert et al., 2018; Kwon et al., 2015; Liu et al., 2020b). For example, aging MPs have been found to cause more severe damage to the grouper liver through the release of acetophenones and benzaldehyde (Wang et al., 2020b). In summary, the aging process changes the physicochemical properties of MPs, further influences the adsorption behavior of contaminants and causes harm to organisms and even humans. Therefore, there is a need to investigate the aging characteristics of MPs and their effects on pollutants in aqueous environments.

Polyvinyl chloride (PVC) plastics are widely used in everyday household products due to their excellent physicochemical properties. The presence of PVC macroscopic and microscopic-size particles is commonly detected in the environment (Wang et al., 2020c). PVC is classified as the most dangerous MPs with strong mutagenicity and carcinogenicity (Wei et al., 2019), in addition to waste PVC or incineration generating toxic intermediates that cause serious environmental pollution (Miao et al., 2020). Therefore, PVC was chosen as a typical MPs in this study. Recent studies have shown that the aging process alters the adsorption of MPs to pollutants, but the correlation between aging characteristics and the adsorption behavior of MPs is unclear. Therefore, sorption capacity and aging characteristics were assessed by adsorption of sulfamethoxazole (SMX) and malachite green (MG), which are hydrophilic organic pollutants frequently detected in surface water and wastewater (Xu et al., 2018; Guo et al., 2019; Tewari et al., 2018; Kadhom et al., 2022; Wang et al., 2023b). The objectives of this study were to (1) reveal the UV aging characteristics of PVC MPs by SEM-Mapping, XRD, FT-IR and 2D-FT-IR-COS; (2) The DOM composition and fluorescence characteristics of MPs leachate were characterized and analyzed by TOC and 3D-EEMs; (3) the changes of particle size, contact angle and molecular weight of MPs during UV aging were investigated; (4) aging indexes were screened from the characterization data to better quantify the surface aging characteristics of MPs, and a correlation model between O/C ratio or CI and aging time was established; (5) the adsorption experiments were conducted to establish the equilibrium adsorption capacity with O/C ratio and mean particle size, and explored the relationship between aging properties of MPs and adsorption capacity. This study will help to better understand the interaction between aging MPs and typical organic pollutants in the aquatic environment, in addition, establish the relationship between aging properties and the adsorption capacity of MPs, and provide a basis for risk assessment of MPs aging.

2. Material and methods

2.1. Materials

Malachite green (MG) (> 98%) and Sulfamethoxazole (SMX) (> 98%) were purchased from Aladdin Industrial Corporation (Shanghai, China). MG was dissolved in deionized water for the preparation of 400 mg/L stock solution. Then the stock solution was kept in the dark. SMX was dissolved in acetonitrile for the preparation of a 10 g/L stock solution. Then the stock solution was kept in the dark at 4 °C. PVC MPs (the mean size 150 μm) was purchased from Tesulang chemical Company (Guangdong, China). All chemicals were used analytical grade or higher purity and solvents were HPLC grade.

2.2. Microplastics aging experiment

UV oxidation is an experimental alternative to the natural aging of MPs that shortens the aging time required in the natural process. The pristine PVC MPs were uniformly placed in glass Petri dishes and aged in a custom-made apparatus (HYR-UV, Mianyang Window Technology Co., Ltd.). Samples were exposed to UV light (6 × 15 W UVC bulb) for 3 d, 7 d, 14 d, 21 d, and 30 d. The UV intensity was 33.97 W/m^2 and the distance from the lamp is 20 cm (Fig. S1). PVC MPs were shaken horizontally every 12 h to ensure uniform exposure. UV-aged PVC MPs with different aging times were obtained. Aging PVC MPs were stored in a dark for subsequent experiments.

2.3. The leaching of aging microplastics

The aged PVC was added to deionized water and sonicated for 10 min. After the leaching was completed, the mixed solution was filtered through a pre-washed GF/F membrane to obtain a plastic-derived DOM sample. All experiments were repeated three times. The three-dimensional excitation-emission matrix (3D-EEM) spectra and concentrations of total organic carbon (TOC) in solution were determined using a fluorescence spectrometer (Shimadzu, RF-6000) and a TOC analyzer (Elementar, Vario), respectively. In the filtration step, a glassware vacuum filtration device was used to avoid direct contact with the samples with foreign plastic materials.

2.4. Adsorption experiments

All adsorption experiments were carried out with brown glass bottles in triplicate to minimize experimental errors. Meanwhile, the blank experiments were conducted under the same conditions as all adsorption experiments to ensure practical accuracy.

The adsorption kinetics experiments were described in Section 1.1 in SI (Supporting Information).

2.5. Analysis of physicochemical characteristics

The remaining MG in the supernatant was analyzed by UV–visible spectrophotometer. The maximum absorption wavelength of MG was 264 nm. The concentration of SMX was measured by high-performance liquid chromatography (HPLC) (Shimadzu LC-20A, Shimadzu, Japan). The injection volume was 20 μL. The measurement wavelength was 269 nm, and the column temperature was set to 30 °C. The flow rate was 1.0 mL/min. The mobile phase consisted of 0.3% formic acid solution and acetonitrile with a ratio of 50:50 (v/v). The retention time of SMX was 6.124 min. The characterization was described in Section 1.2 in SI.

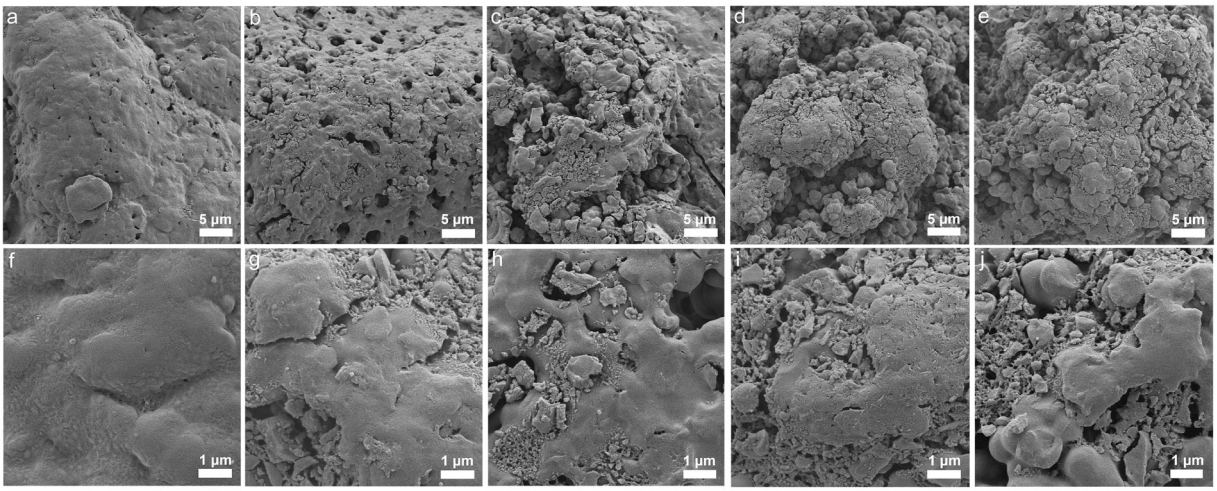

Fig. 1. SEM images of PVC MPs with UV aging (a, f) 0 d; (b, g) 7 d; (c, h) 14 d; (d, i) 21 d; (e, j) 30 d.

3. Results and discussion

3.1. The characterization of PVC MPs

3.1.1. Surface morphology

The morphological changes of MPs are an essential indicator of their aging degree to explore the aging mechanism of MPs during UV aging. The surface morphology of MPs under different UV irradiation is depicted in Fig. 1. We can see that the surface of the pristine

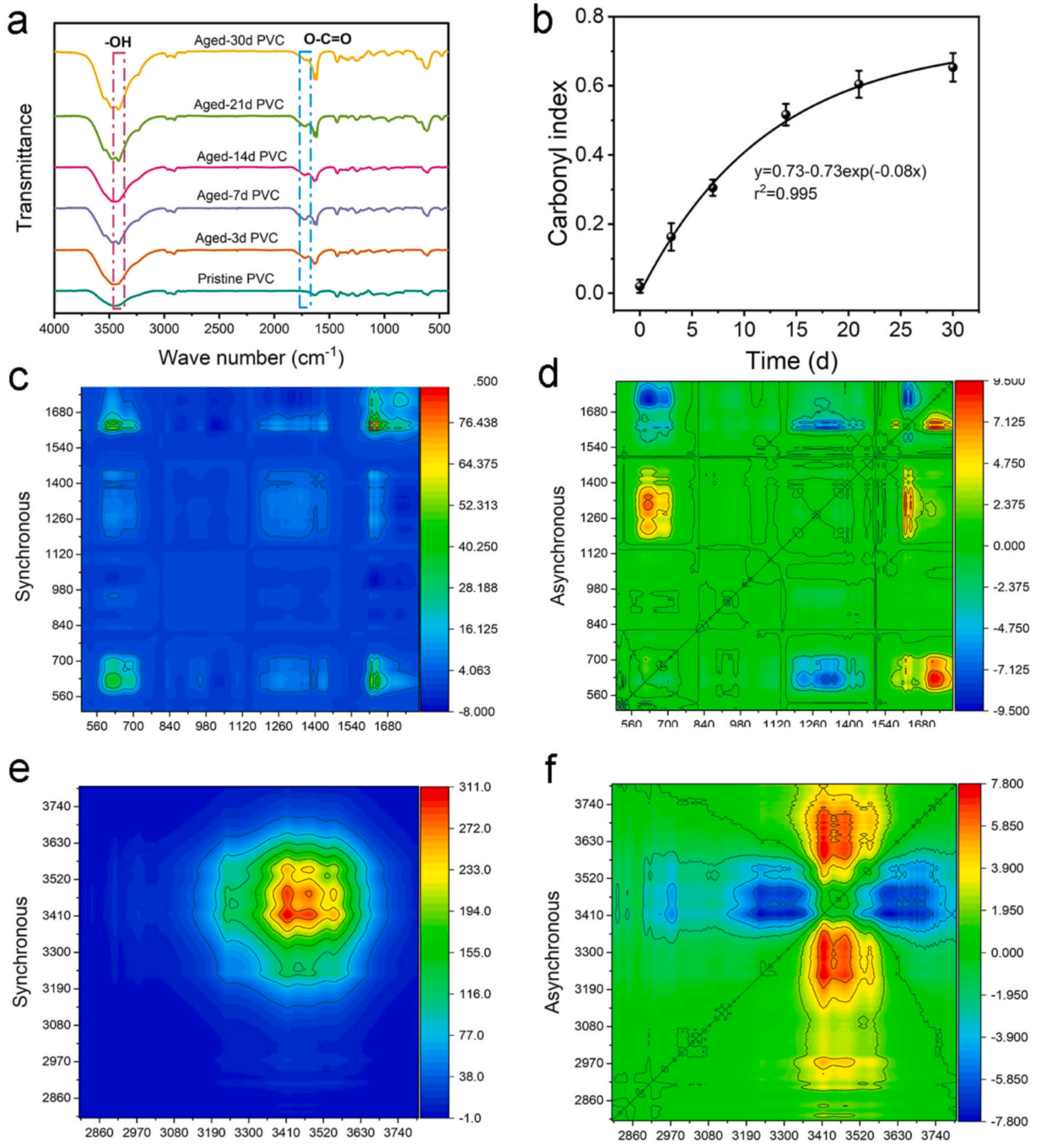

Fig. 2. (a) FT-IR spectra of PVC MPs with different aging times; (b) Variations of carbonyl index PVC MPs at the different aging times; (c-d) Synchronous and asynchronous maps of two-dimensional correlation spectroscopy (2D-COS) based on FT-IR spectra in 500–1800 cm^{-1} and (e-f) 950–1950 cm^{-1} regions.

PVC is relatively smooth, and with the increase of aging time, the surface gradually becomes rough, with more cracks and flakes on the surface and debris attached, which may be mainly due to the difference of the nature and brittleness of PVC MPs.

3.1.2. FTIR analysis

To further investigate the response of extended UV aging time to the structural changes of MPs, FT-IR spectroscopy and 2D-FTIR-COS were applied to monitor the subtle changes of surface functional groups of MPs during aging. As exhibited in Fig. 2, for the pristine PVC MPs the transmission of absorption peaks at 3446 and 1716 cm^{-1} was relatively weak, indicating that the pristine PVC MPs contained a small amount of hydroxyl and carbonyl groups, and this result was consistent with the XPS results. However, the transmittance gradually increased with the increase of UV irradiation time, indicating that the content of functional groups gradually increased after aging. In addition, the newly formed hydroxyl and carbonyl groups indicate that the aging MPs underwent oxidation reactions with different hydrophilicity. After photoaging, three absorption bands appeared at around 1610 cm^{-1}, 1716 cm^{-1} and 3300–3600 cm^{-1}, representing the stretching vibration peaks of -C═C-, -C═O and -OH, respectively (Fig. 2a). The appearance of carbon-carbon double bond, carbonyl and hydroxyl absorption peaks and the increase of their peak intensities indicate that dichlorination and photoreduction reactions occur during UV irradiation, and the absorption peaks gradually increase with the increase of aging time.

The concept of carbonyl index (CI) has been used in many papers to quantify the aging of MPs. The carbonyl index is defined as the ratio of the carbonyl peak intensity to the reference peak intensity. In this study, the carbonyl peak was located at 1716 cm^{-1} and the reference peak was chosen to be consistent with previous literature by choosing the peak at 2910 cm^{-1}, which is the asymmetric stretching vibration peak of methylene. Fig. 2b shows the variation of CI for PVC MPs with different aging times. The figure shows a slightly S-shaped CI curve, which increases and then decreases, implying that the rate of change of CI increases and then decreases, which means there is an initiation process of UV aging of PVC, that accelerates after initiation and slows down after aging to a certain degree, and such a trend of change provides a basis for determining the aging mechanism of PVC afterward.

In order to follow the subtle changes in PVC MPs during the aging process, 2D-COS analysis was used to resolve the FT-IR spectra. The 2D-FT-IR-COS plots (synchronous and asynchronous) of PVC MPs at different aging times are shown in Fig. 2c-f. In the 2D-COS spectra, the peaks on the diagonal are called auto peaks and the peaks outside the diagonal are called cross peaks. Based on FT-IR spectra, the regions of 500–1800 cm^{-1} and 2800–3800 cm^{-1} were selected for 2D-FT-IR-COS analysis of PVC. According to the synchro grams, five auto peaks were observed at diagonals 604, 1250, 1435, 2911 and 3446 cm^{-1}, corresponding to the characteristic peaks of C-Cl, Cl-CH_2, Cl-CH, C-H and O-H, respectively. In the synchronous map, all cross peaks are positive signals, indicating that most of the functional groups underwent synchronous changes (decrease in peak intensity) during the aging process. The asynchronous mapping is about diagonal antisymmetry and represents only the asynchrony between two wave numbers. Therefore, only the cross-peaks are present.

According to Noda's law (Text S4), asynchronous correlation spectra can reveal the order of changes in functional groups during aging. It can be seen from the asynchronous plot that there are significant differences in the cross-peak signals, especially for oxygen-containing functional groups such as H-C═O, O-C═O, and O-H. As can be seen from the Table 1, the cross-peak at ψ (2911, 3446) is negative, indicating that the band change order at 3446 cm^{-1} is preceded by that at 2911 cm^{-1}. In addition, the reaction order varies more among different functional groups in the lower band of 500 ~ 1800 cm^{-1}. As presented in Table 1, the cross peaks of ψ (x1, 1740), ψ (x2, 1663), ψ (x3, 1435), and ψ (x4, 1250) are all negative, indicating that the reaction order of different functional groups in the range of 500–1800 cm^{-1} is: 604 (C-Cl) > 1250 (Cl-CH_2) > 1435 (Cl-CH) > 1610 (H-C═O) > 1716 (O-C═O).

3.1.3. XPS and contact angle analysis

From the XPS spectra, peaks (corresponding to C 1 s and O 1 s) were observed at 284.9 eV and 532 eV for pristine PVC MPs (Fig. 3), indicating that oxidation also occurred on the surface of pristine PVC MPs. While for the O 1 s peaks of PVC MPs with different aging times, the intensity increases with the aging time. To clearly show the aging degree of MPs, we investigated the oxygen-to-carbon atom ratio (O/C) of PVC MPs with different aging times and tried to model the relationship between the O/C ratio and aging time. As exhibited in Fig. 4a, the relationship between the O/C ratio and aging time of PVC MPs can be described by an exponential equation, and the rate of change can be well-fitted by pseudo-first-order kinetics ($r^2 = 0.997$), with the most significant changes in the first 21

Table 1
The 2D-COS data on the assignment and sign of each cross-peak in synchronous and asynchronous (in the brackets) maps of aged PVC treated by UV irradiations.

Peak (cm^{-1})	Band assignments	Sign						
		604	1250	1435	1610	1716	2911	3446
604	C-Cl	+	+ (-)	+ (-)	+ (-)	+ (-)	+	+
1250	Cl-CH_2		+	+ (-)	+ (-)	+ (-)	+	+
1435	Cl-CH			+	+ (-)	+ (-)	+	+
1610	H-C═C				+ (-)	+ (-)	+	+
1716	C═O				+	+	+	+
2911	C-H						+	+ (-)
3446	O-H							+

Note: (1) " + " and " - " represents the positive sign and negative sign, respectively. (2) The order of signs in/out of the brackets represents the conditions of aging by UV irradiations. (3) All the signs were obtained in the bottom-right parts of the 2D maps.

days and smaller changes thereafter. This finding may be attributed to the availability of active sites on the surface of MPs.

At the beginning of UV aging, the excess of free radicals led to the rapid oxidation of the MPs surface. However, as the reaction proceeds, the effective adsorption sites gradually decrease and the surface oxidation becomes saturated, which explains the plateauing of the O/C ratio of PVC MPs with increasing aging time. the natural weathering process of MPs may exhibit a similar phenomenon in the surface aging properties, as sunlight or heat is sustainable.

As mentioned earlier, the increase in the O/C ratio and CI values in PVC MPs slowed down with increasing aging time. It can be seen from the fitted relationship between the O/C ratio and CI versus aging time: $r^2(O/C) = 0.968 < r^2(CI) = 0.995$, which may be due to the difference between XPS and FTIR analysis techniques, where XPS allows surface analysis at nanometer thickness, while FTIR probes micrometer depth. Since the oxidation reaction starts at the polymer surface, the internal oxidation of MPs takes a longer time. Indeed, the simplicity of operation and the low cost of FTIR techniques have led to the widespread use of CI in characterizing polymer aging. In contrast, natural aging processes, especially UV irradiation, are mostly confined to the surface and limited by the penetration of light and diffusion of oxygen within the polymer. Therefore, the CI values may not fully reflect the changes in the surface aging properties. So, the XPS measurements can be used as a complementary tool to detect the surface aging properties of MPs. O/C ratios can cover oxygen functional groups (e.g., C-O and O-H) that may not be included in the CI values, and high-resolution XPS spectra provide detailed information about the polymer surface. Overall, the aging behavior of MPs can be evaluated more comprehensively based on O/C and CI parameters.

In addition, the water contact angle of MPs with different aging times were tested, and the contact angle results showed that the pristine PVC MPs were highly hydrophobic with a contact angle of 143.3°, while the UV aging treatment significantly reduced the contact angle of MPs. After 30 d of UV aging treatment, the contact angle of PVC decreased to 105.6°, indicating that the oxidation process could improve the hydrophilicity of MPs. In addition, the contact angle of PVC maintained a high rate of decrease throughout the oxidation stage. To clearly show the aging degree of MPs, we investigated the contact angle of PVC MPs with different aging times versus aging time as well as O/C ratio and CI, and tried to simulate the relationship (Fig. 4b, c and e). It can be seen from the plots that

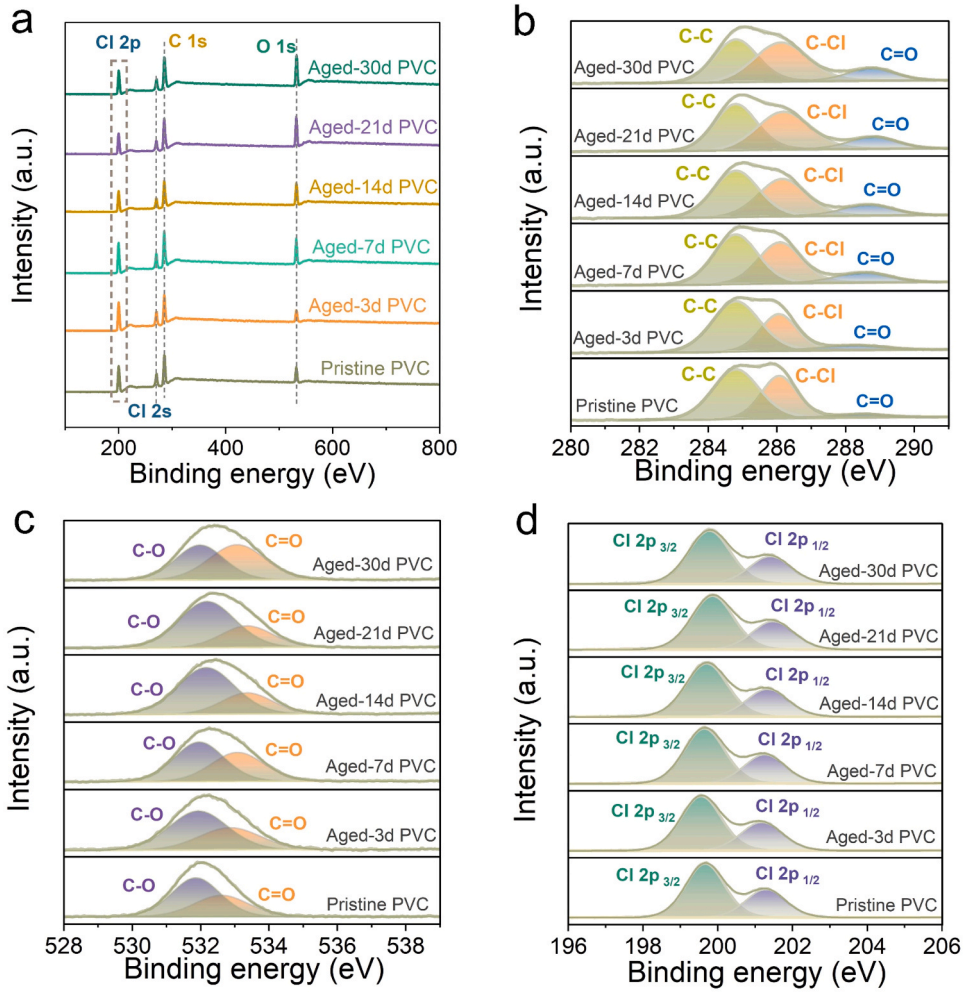

Fig. 3. (a) XPS survey scan; (b) C 1 s; (c) O 1 s and (d) Cl 2p spectra for PVC and PVC aged for different days.

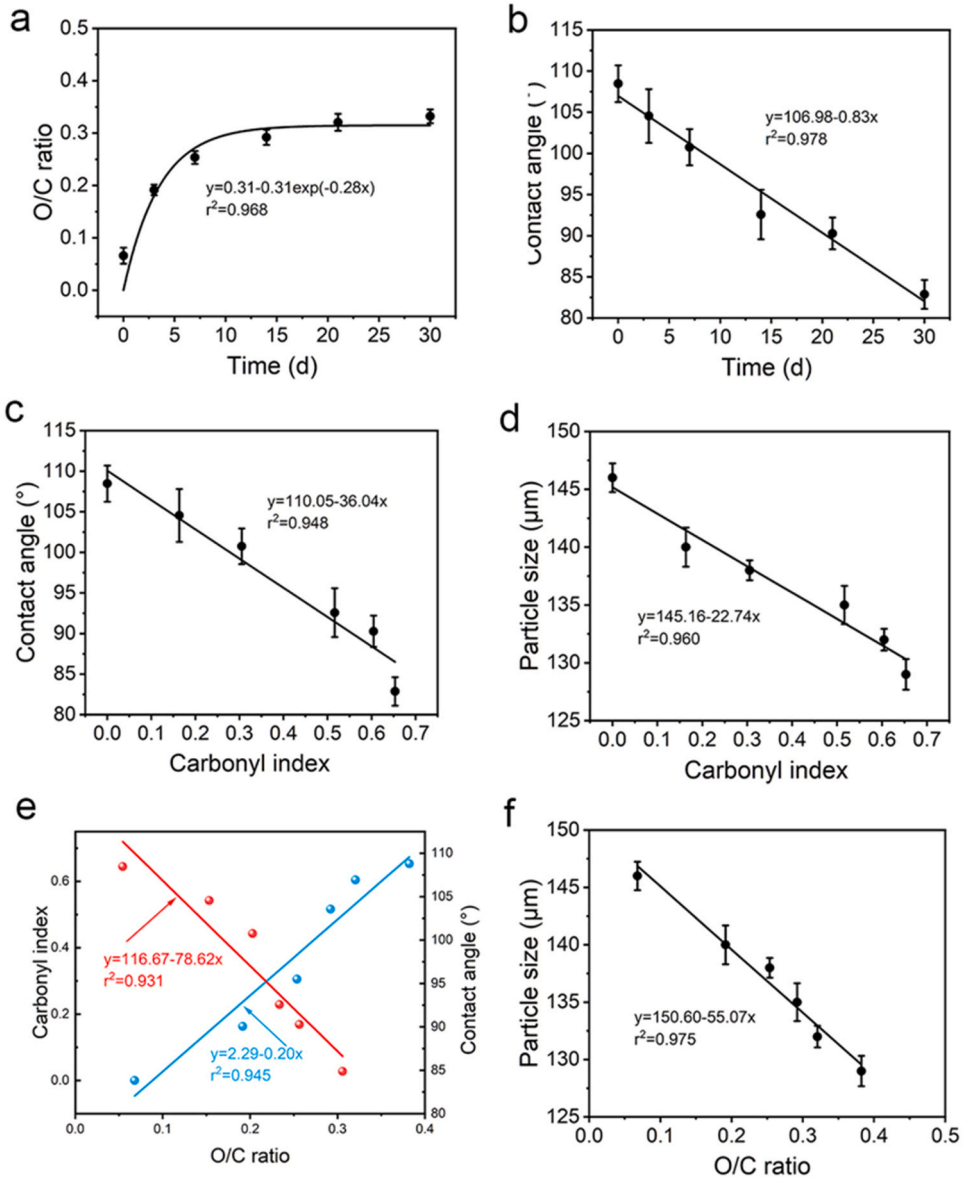

Fig. 4. (a) Correlations between O/C ratio and aging time; (b) Correlations between contact angle and aging time; (c) Correlations between contact angle and CI; (d) Correlations between particle size and CI; (e) Correlation of CI or contact angle with O/C ratio; (f) Correlations between particle size and O/C ratio. The color of each equation corresponds with the same color of the symbol and line.

the contact angles of PVC MPs with different aging times were linearly correlated with the aging time, CI, and O/C ratio, respectively ($r^2 = 0.978$, $r^2 = 0.948$, $r^2 = 0.931$). The contact angle decreases with increasing aging time, which is mainly due to the increase of oxygen-containing functional groups, which make the PVC surface more hydrophilic.

3.1.4. XRD and Zeta potential analysis

Fig. S2a shows the XRD spectra of PVC MPs before and after UV aging. It is observed that the intensity of the characteristic peaks of the aged PVC increased slightly than that of the pristine PVC, and the crystallinity of the aged PVC strengthen slightly. The amorphous polymers are preferentially degraded in aging, which increases the crystallinity. At the same time, as the physical integrity of MPs is destroyed with the prolongation of UV aging time, their surface chemistry characteristics may also change, which leads to a change in crystallinity.

From the Fig. S2b, we can see that the Zeta potential decrease with increasing aging time, which is mainly due to the increase of oxygen-containing functional groups. At the same time, they are easily deprotonated and negatively charged in an aqueous environment, thus increasing the adsorption capacity of hydrophilic pollutants.

3.1.5. Particle size and Molecular weight distribution analysis

The distribution of the particle size changes of PVC MPs with different aging times is shown in Fig. 5a. The proportion of pristine PVC MPs with particle size ≥ 150 μm was 78.6%, and the main particle size was 140 ~ 150 μm. And after 30 d of UV aging treatment, the particle size of PVC MPs with different aging times was gradually reduced, D(4, 3) denotes the volume average diameter, and after aging, the volume average particle size changed to aging (30 d) = 129 μm, aging (21 d) = 132 μm, aging (14 d) = 135 μm, aging (7 d) = 138 μm, aging (3 d) = 140 μm, pristine = 146 μm, indicating that MPs underwent significant fragmentation during the oxidation process and the particle size gradually decreased.

The specific changes in the long-chain structure, molecular weight and molecular weight distribution of PVC MPs with different aging times were further analyzed using the GPC method, as presented in Fig. 5b. It can be seen from the figure that the number-average molecular weight Mn of PVC MPs decreased sharply after aging, indicating that the chain-breaking reaction increased the number of low-molecular-weight molecular chains, and the weight-average molecular weight M_w and other molecular weight changes showed the same trend. The larger polydispersity index (PDI) of aged PVC MPs indicates that the aging process increases the heterogeneity of PVC MPs (Table 3), suggesting that the aging process increases the width of the molecular weight distribution. In Fig. S3, the GPC peaks of the aged 14 d PVC MPs shifted to higher retention volumes and had higher detector response or refractive index (RI) compared to the original samples, indicating that the aging process resulted in lower molecular weights and higher concentrations than the pristine PVC MPs. With the increase in aging time, the GPC peak shifted to a higher retention volume and the GPC peak broadened and decreased significantly, confirming that the molecular chain breakage of PVC MPs occurred during aging.

3.2. Leaching analysis

To investigate the leachate of PVC MPs during UV aging, the content of dissolved organic matter in the solution was determined by the TOC method, thus examining the decomposition of polymer chains during UV aging. As exhibited in Fig. S4a, the TOC content in the leachate of PVC MPs with different aging times gradually increased, and its concentration reached 98.5 ± 3.53 mg/L after 30 d of UV irradiation. To clearly show the decomposition of PVC MPs with different aging times during UV aging, we investigated the relationship between the TOC content in the leachate of PVC MPs and the aging time, moreover tried to simulate the correlation between TOC content and aging time. In Fig. S5b, it can be seen that the TOC content of PVC MPs with different aging times showed a good fit by pseudo-first-order model ($r^2 = 0.997$).

It has been demonstrated that the absorbance at 220–280 nm of UV-Vis spectrophotometry is most suitable for the analysis of NOM, and different wavelengths of light sources can identify different chromophores in NOM. Among them, UV_{254} is the more widely used parameter, which is generally considered to reflect the content of aromatic compounds in NOM and has a greater practical value. From Fig. S5, we can see that the absorbance in the leachate of PVC MPs with different aging times gradually increased at the wavelength of UV_{254} with the extension of aging time, indicating that a large amount of unsaturated conjugated double bonds and aromatic chemicals are produced during the UV aging process. In addition, specific UV absorbance (SUVA) is the ratio of the absorbance of the water sample at 254 nm to its dissolved organic matter (DOC) content. From Fig. S4b, we can see that the SUVA values in the leachate of PVC MPs with different aging times gradually increased as the aging time was prolonged. However, after 15 days, it tends to level off as the aging time increases. This is consistent with the trend of the CI index as well as the O/C ratio. The water samples with larger SUVA values contained more hydrophobic organic matter, especially aromatic organic matter, while the water samples with smaller SUVA values contained more hydrophilic organic matter. To clearly show the decomposition of MPs in solution with different aging times, we studied the relationship between the SUVA and aging time in the leachate of PVC MPs, and tried to simulate the relationship between the SUVA and aging time. Moreover, it can be seen that the SUVA in the leachate of PVC MPs with different aging times showed a good fit by pseudo-first-order model ($r^2 = 0.922$) with the aging time.

In addition, 3D-EEM spectra can effectively reflect the characteristics of the fluorescent material composition during UV aging, and the leaching composition was investigated using 3D-EEM. The EEMs of PVC leaching under different aging conditions were plotted (Fig. 6). Several peaks appeared in the protein-like fluorescence spectral region. This region is defined as peak B (−225 (−280)/

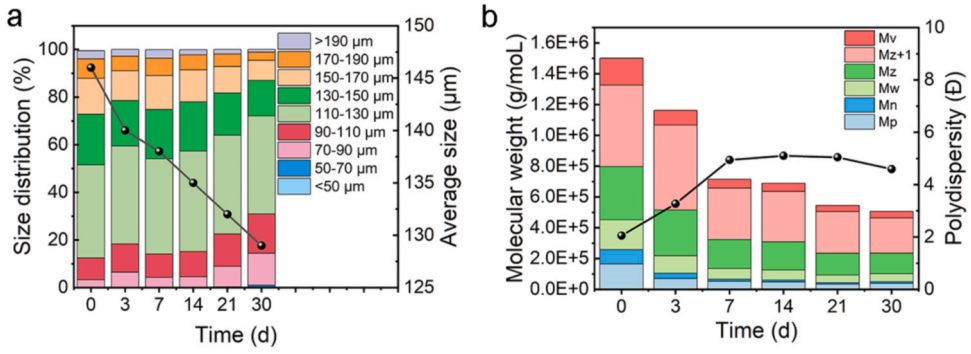

Fig. 5. (a) Size distribution and an average size of PVC MPs aged for different days; (b) Molecular weight and polydispersity of PVC MPs aged for different days.

− 305 nm) and peak T (−225 (−280)/− 350 nm), representing tyrosine-like and tryptophan-like substances. Interestingly, in the leachate of PVC MPs after 7 days under UV aging, the protein or phenolic fluorescence intensity showed a decreasing trend with increasing UV irradiation time, which may be the result of photolytic degradation of the fluorescent groups. And additional peaks appeared in the humic acid-like fluorescence region, defined as the A-peak (250–300/400–450 nm). The fluorescence intensity gradually increased with increasing aging time, indicating a gradual increase in humic substance concentration. Thus, these results seem to link the appearance of humic acid-like substances to the effect of UV irradiation. The change of EEM distribution is due to the small molecules produced by the breaking of molecular chains during the aging process, and the release of additives contained in the microplastics themselves. Moreover, due to the presence of DOM, the aging of PVC MPs is aggravated, making the change of EEM distribution gradually obvious.

The compositional characteristics in the leachate of PVC MPs with different aging times were further quantitatively resolved by FRI (fluorescence region volume integral). From Fig. S6b. It was found that with the increase of aging time, region IV was protein-like substances related to microbial metabolism, and the fluorescence region volume integral gradually decreased from 40.16% to 2.34%, while region V was humic acid-like substances, and the fluorescence region volume integral gradually increased from 59.84% to 97.66%, and the results were consistent with the 3D-EEM fluorescence results. In addition, we observed three fluorescence characteristic indices, including fluorescence index (FI), humification index (HIX) and biogenic index (BIX), and FI, BIX and HIX could effectively indicate the aromaticity and humification degree of DOM. Generally, when FI $<$ 1.4 or BIX $<$ 0.6 or HIX $>$ 10, it indicates that the aromaticity and humification degree of DOM is high; when FI $>$ 1.7 or BIX $>$ 1 or HIX $<$ 4, it indicates that the aromaticity and humification degree of DOM is low. As can be seen from the Table. S3, the FI, BIX and HIX values of leachate fractions of PVC MPs with different aging times ranged from 0.79 to 1.84, 0.25–1.55 and 0.21–20.40, respectively, indicating that the leachate fractions of PVC MPs with different aging times were mainly composed of organic matter with higher aromaticity and a higher degree of humification (Fig. S6a). The FI and BIX of the components basically showed a sequential decreasing trend, while the HIX values showed an increasing trend. The results indicated that the leachate fractions of PVC MPs were enriched with more organic components with high aromaticity and a high degree of humification with the increase of aging time.

Furthermore, in order to give a clearer picture of the aging mechanism of PVC MPs, we determined the chloride ion content in the aging filtrate. As shown in Fig. S7, the dehydrochlorination reaction of PVC MPs was rapid in the UV irradiation, and the concentration of released Cl^- significantly increased from 0.23 mg/L to 32.53 mg/L as the illumination time was prolongated from 0 d to 30 d. During the photodegradation process, the dehydrochlorination reaction occurred to generate conjugated polyene and hydrogen chloride (HCl). The dehydrochlorination reaction is an important photoreduction process in the photoaging of PVC MPs, which

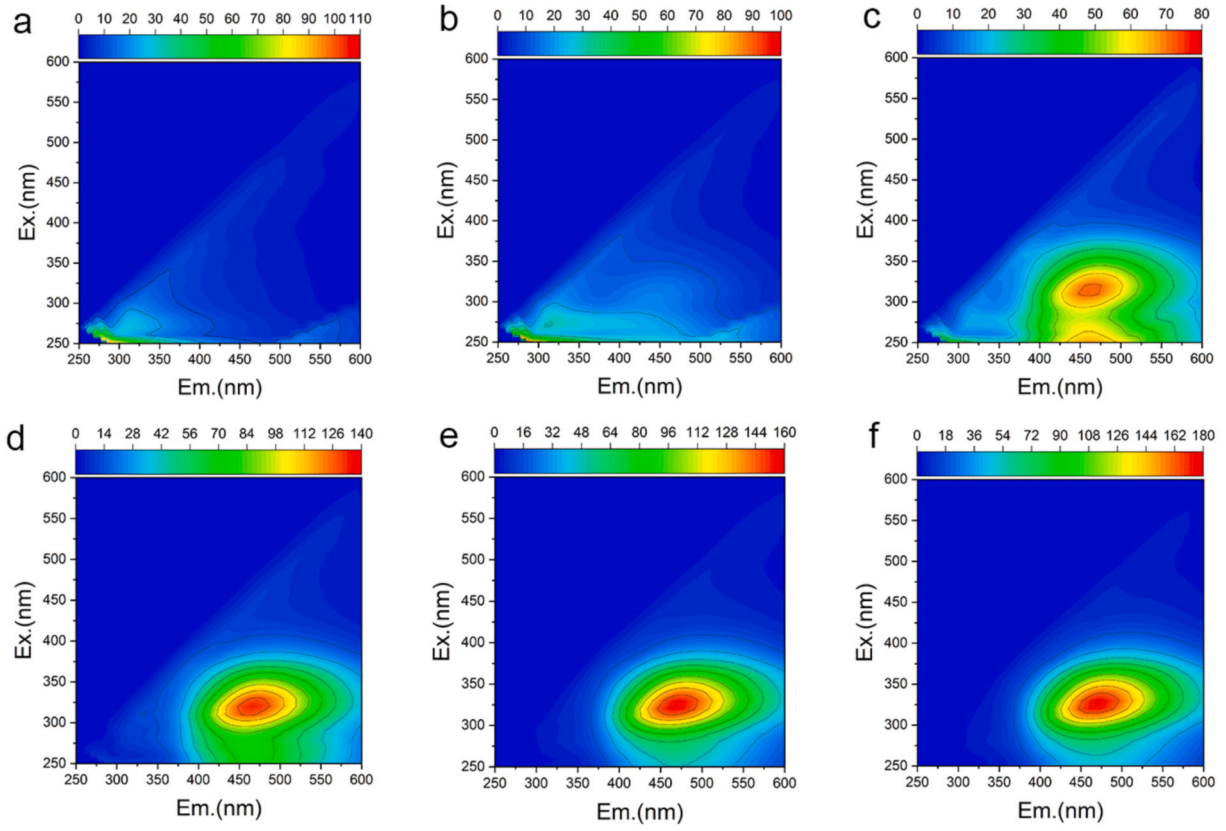

Fig. 6. Fluorescence EEM plots of the DOM leached from the PVC MPs with UV aging (a) 0 d; (c) 7 d; (d) 14 d; (e) 21 d; (f) 30 d.

changes its light absorption properties. The color of aged PVC MPs gradually shifted from white to yellow, due to the formation of the conjugated polyene structure.

3.3. Effect of UV aging on the adsorption capacity of PVC MPs

The adsorption capacity of SMX and MG by PVC MPs with different aging times versus the adsorption time is shown in Fig. S8. It can be seen that the adsorption showed a trend of fast and then slow, finally tended to dynamic equilibrium in the process of SMX adsorption by PVC MPs (Fig. S8a). The adsorption process is mainly divided into three stages: for the pristine PVC MPs, the first 6 h of adsorption is a fast process, followed by a slow stage at 12 h. The dynamic adsorption equilibrium is basically reached at 24 h, and the equilibrium adsorption amount is 0.168 mg/g; while for the PVC MPs with different aging times, the first 12 h of adsorption is a fast process, followed by a slow stage at 12 h, and the dynamic adsorption equilibrium is basically reached at 48 h. The equilibrium adsorption amounts were 0.214 mg/g (Aged 3 d), 0.240 mg/g (Aged 7 d), 0.265 mg/g (Aged 14 d), 0.281 mg/g (Aged 21 d) and 0.290 mg/g (Aged 30 d), respectively. In addition, from the plots of SMX adsorption by PVC MPs with different aging times versus aging time, we found a linear correlation between the adsorption amount and aging time, CI and O/C ratio, respectively ($r^2 = 0.923$, $r^2 = 0.995$, $r^2 = 0.960$) (Fig. S9a, b, c). For MG, the relationship between the effect of time on the adsorption of MG by PVC MPs is shown in Fig. S8b. It was found that the adsorption process showed a trend of fast and then slow and finally tended to dynamic equilibrium. The adsorption process was divided into three main stages: for both pristine and aged PVC MPs the first 12 h of the reaction was a fast process, followed by a slow stage at 36 h. The dynamic adsorption equilibrium was basically reached at 48 h. The equilibrium adsorption amounts were 2.107 mg/g (Pristine), 4.579 mg/g (Aged 3 d), 7.307 mg/g (Aged 7 d), 9.808 mg/g (Aged 14 d), 11.890 mg/g (Aged 21 d) and 12.933 mg/g (Aged 30 d), respectively. And from the graphs of the adsorption of MG by PVC MPs versus aging time, it can be seen that the adsorption capacity of MG by PVC MPs gradually increased with the increase of aging time, and the adsorption amount was linearly correlated with aging time, CI and O/C ratio, respectively ($r^2 = 0.991$, $r^2 = 0.940$, $r^2 = 0.989$) (Fig. S9d, e, f). The analysis is mainly due to the increase of oxygen-containing functional groups of PVC microplastics after aging, which become more hydrophilic (Fig. 7). And the specific adsorption mechanism is explained as follows:

For the adsorption of MG by PVC MPs, from Fig. S1b, we can see that the zeta potential of PVC MPs gradually decreases with the aging time, indicating a higher negative electronegativity of PVC MPs. Furthermore, the p*K*a of MG is 5.62 ± 0.24, having a positive electrical charge. Hence, an electrostatic attraction could happen between MG and PVC MPs, and its intensity increases as the difference in the charges increases; For the adsorption of SMX, from Fig. S10b, we can obtain that SMX is predominantly negatively charged at pH = 7. Moreover, PVC MPs is known for its high negative charge. Hence, an electrostatic discharge could happen between SMX and PVC MPs, and its intensity increases as the difference in the charges increases. However, the results of adsorption experiments showed a gradual increase in adsorption with aging time, thus indicating that hydrogen bonding is the main mechanism for the adsorption process of SMX on PVC MPs.

After SMX and MG were adsorbed on PVC MPs, the samples were analyzed using FTIR, respectively, which could better explain the

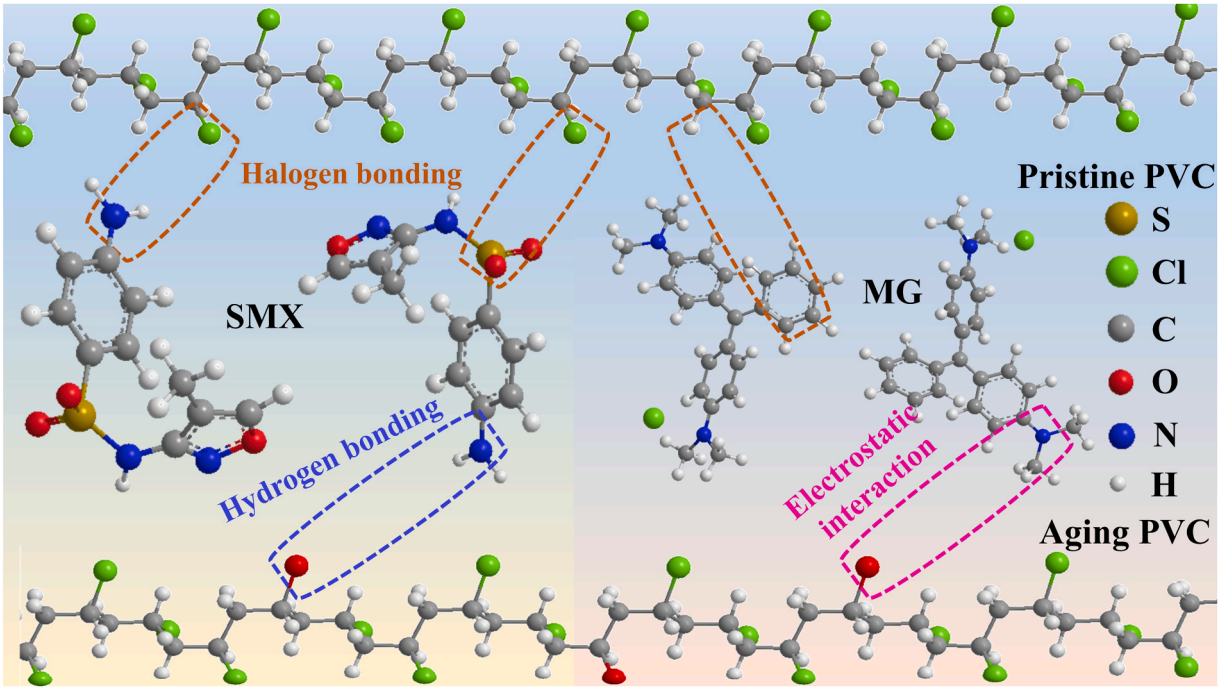

Fig. 7. Schematic diagram of the adsorption mechanism of SMX and MG on PVC MPs before and after aging.

interaction mechanisms between PVC MPs and targeted pollutants. As depicted in Fig. S11a, the -C═O characteristic peak at 1720–1600 cm^{-1} changed significantly after the aged PVC MPs adsorbed MG, which proved that -C═O interacted with MG. Furthermore, after the aged PVC MPs adsorbed MG, the stretching vibration peak of -O–H showed significant changes, and the peak area of -O–H decreased. This might be because the adsorption of MG on -C-OH. Thus, indicating the dominance of electrostatic action in this adsorption process; For the adsorption of SMX, From Fig. S11b, we can obtain that the carboxyl broad peaks at the vicinity of 3400 cm^{-1} were diminished after sorption. Therefore, the carboxyl groups were involved in the adsorption. Moreover, the peak -C═O at 1720–1600 cm^{-1} was attenuated to various extents after adsorption. It expressed the carboxyl and amide groups of SMX were engaged in the sorption. The above suggested that hydrogen bonding played an essential role in the adsorption process. The formation of hydrogen bonds might be the main mechanism of SMX on PVC MPs.

As mentioned previously, the average particle size and O/C ratio can reflect the aging properties of MPs. Since the O/C ratio was linearly correlated with CI or contact angle and the mean particle size was linearly correlated with specific surface area, we established the relationship between equilibrium adsorption capacity (Q_e) with O/C ratio and mean particle size to evaluate the correlation between the aging properties and adsorption capacity of MPs. In the correlation analysis, reasonable correlations between Q_e (SMX, eq 1) and Q_e (MG, Eq. 2) with the O/C ratio and mean particle size of PVC MPs were found, as follows.

$$y = 0.143x_1 - 0.002x_2 + 0.385, r^2 = 0.996 \quad (1)$$

$$y = 2.670x_1 - 0.963x_2 + 121.591, r^2 = 0.998 \quad (2)$$

where y is the equilibrium adsorption capacity of Q_e (mg/g), x_1 is the O/C ratio, and x_2 (μm) is the average particle size.

Notably, the linear relationship between Q_e with O/C ratio and mean particle size indicates that O/C ratio and mean particle size have a significant effect on the equilibrium adsorption capacity. It has been previously documented that the introduction of oxygen-containing groups can increase the polarity and hydrophilicity of polymers, which may facilitate the interaction between PVC MPs on SMX and MG molecules. The linear relationship between particle size and specific surface area further suggests that the adsorption of MPs is related to the surface adsorption sites of MPs. While the artificially accelerated aging processes of the MPs in the current study are far from the actual situation, it provides an opportunity to study the correlation between the aging performance of MPs and the sorption capacity of MPs in the environment. It is also interesting to note that compared to the O/C ratio, CI values are also suitable for constructing the relationship between Q_e and aging properties, probably because CI may also represent the role of hydrophilicity in the process of adsorption, as shown by the best linear correlation between CI and contact angle.

4. Conclusions

The aim of this study was to accelerate the degree of aging of PVC MPs by UV irradiation in order to improve understanding of their long-term aging behavior in the natural environment. In summary, our results suggest that the surface morphology, particle size, contact angle, and molecular weight of the PVC MPs were found to change significantly with the UV aging time by characterizations. And it was found by filtrate analysis that as the aging time increased, the content of TOC and humic acid-like substances gradually increased. Moreover, we obtained the O/C ratio can be used as a proxy parameter for the CI value to quantify the surface aging properties of PVC MPs and propose the correlation model between the adsorption capacity with the O/C ratio or CI and the mean size. This model is an attempt to elucidate the relationship between aging properties and aging time/adsorption behavior of MPs, which helps to address the MPs contamination problem more comprehensively.

CRediT authorship contribution statement

Kefu Wang: Conceptualization, Methodology, Validation, Formal analysis, Investigation, Data curation, Writing – original draft, Writing – review & editing, Visualization. **Kangkang Wang:** Validation, Formal analysis, Writing – review & editing. **Siqi Liang:** Investigation, Formal analysis. **Changyan Guo:** Methodology, Resources, Investigation, Formal analysis, Writing – review & editing, Visualization. **Wei Wang:** Project administration, Funding acquisition., Writing – review & editing. **Jide Wang:** Writing – review & editing Supervision, Project administration, Funding acquisition.

Declaration of Competing Interest

The authors declare that they have no known competing financial interests or personal relationships that could have appeared to influence the work reported in this paper.

Data Availability

Data will be made available on request.

Acknowledgments

This research was financially supported by the National Natural Science foundation of China (Grant No. 32061133005) and the

Research Council of Norway (RCN, project 320456).

Appendix A. Supporting information

Supplementary data associated with this article can be found in the online version at doi:10.1016/j.eti.2023.103405.

References

Alimi, O.S., Farner Budarz, J., Hernandez, L.M., Tufenkji, N., 2018. Microplastics and nanoplastics in aquatic environments: aggregation, deposition, and enhanced contaminant transport. Environ. Sci. Technol. 52, 1704–1724.

Anastopoulos, I., Pashalidis, I., Kayan, B., Kalderis, D., 2022. Microplastics as carriers of hydrophilic pollutants in an aqueous environment. J. Mol. Liq. 350, 118182.

Andrady, A.L., 2011. Microplastics in the marine environment. Mar. Pollut. Bull. 62, 1596–1605.

Andrady, A.L., 2015. Persistence of Plastic Litter in the Oceans. In: Bergmann, M., Gutow, L., Klages, M. (Eds.), Marine Anthropogenic Litter. Springer International Publishing, Cham, pp. 57–72.

Chae, Y., An, Y.-J., 2018. Current research trends on plastic pollution and ecological impacts on the soil ecosystem: A review. Environ. Pollut. 240, 387–395.

Chen, G., Feng, Q., Wang, J., 2020. Mini-review of microplastics in the atmosphere and their risks to humans. Sci. Total Environ. 703, 135504.

Duncan, E.M., Broderick, A.C., Fuller, W.J., Galloway, T.S., Godfrey, M.H., Hamann, M., Limpus, C.J., Lindeque, P.K., Mayes, A.G., Omeyer, L.C.M., Santillo, D., Snape, R.T.E., Godley, B.J., 2019. Microplastic ingestion ubiquitous in marine turtles. Glob. Change Biol. 25, 744–752.

Frias, J.P.L., Nash, R., 2019. Microplastics: finding a consensus on the definition. Mar. Pollut. Bull. 138, 145–147.

Frias, J.P.L., Otero, V., Sobral, P., 2014. Evidence of microplastics in samples of zooplankton from Portuguese coastal waters. Mar. Environ. Res. 95, 89–95.

Galgani, L., Engel, A., Rossi, C., Donati, A., Loiselle, S.A., 2018. Polystyrene microplastics increase microbial release of marine chromophoric dissolved organic matter in microcosm experiments. Sci. Rep. 8, 14635.

Galloway, T.S., Cole, M., Lewis, C., 2017. Interactions of microplastic debris throughout the marine ecosystem, Nat. Ecol. Evol. 1, 0116.

Gardette, M., Perthue, A., Gardette, J.-L., Janecska, T., Földes, E., Pukánszky, B., Therias, S., 2013. Photo- and thermal-oxidation of polyethylene: comparison of mechanisms and influence of unsaturation content. Polym. Degrad. Stab. 98, 2383–2390.

Gewert, B., Plassmann, M.M., MacLeod, M., 2015. Pathways for degradation of plastic polymers floating in the marine environment. Environ. Sci. Process. Impacts 17, 1513–1521.

Gewert, B., Plassmann, M., Sandblom, O., MacLeod, M., 2018. Identification of chain scission products released to water by plastic exposed to ultraviolet light. Environ. Sci. Technol. Lett. 5, 272–276.

Guo, X., Chen, C., Wang, J., 2019. Sorption of sulfamethoxazole onto six types of microplastics. Chemosphere 228, 300–308.

Guo, X., Hu, G., Fan, X., Jia, H., 2020. Sorption properties of cadmium on microplastics: the common practice experiment and A two-dimensional correlation spectroscopic study. Ecotoxicol. Environ. Saf. 190, 110118.

Hanun, J.N., Hassan, F., Jiang, J.-J., 2021. Occurrence, fate, and sorption behavior of contaminants of emerging concern to microplastics: influence of the weathering/aging process. J. Environ. Chem. Eng. 9, 106290.

Hu, B., Li, Y., Jiang, L., Chen, X., Wang, L., An, S., Zhang, F., 2020. Influence of microplastics occurrence on the adsorption of 17β-estradiol in soil. J. Hazard. Mater. 400, 123325.

Huang, D., Xu, Y., Yu, X., Ouyang, Z., Guo, X., 2021. Effect of cadmium on the sorption of tylosin by polystyrene microplastics. Ecotoxicol. Environ. Saf. 207, 111255.

Jahnke, A., Arp, H.P.H., Escher, B.I., Gewert, B., Gorokhova, E., Kühnel, D., Ogonowski, M., Potthoff, A., Rummel, C., Schmitt-Jansen, M., Toorman, E., MacLeod, M., 2017. Reducing uncertainty and confronting ignorance about the possible impacts of weathering plastic in the marine environment. Environ. Sci. Technol. Lett. 4, 85–90.

Jiang, H., Zhang, Y., Bian, K., Wang, C., Xie, X., Wang, H., Zhao, H., 2022. Is it possible to efficiently and sustainably remove microplastics from sediments using froth flotation? Chem. Eng. J. 448, 137692.

Jiang, H., Bu, J., Bian, K., Su, J., Wang, Z., Sun, H., Wang, H., Zhang, Y., Wang, C., 2023. Surface change of microplastics in aquatic environment and the removal by froth flotation assisted with cationic and anionic surfactants. Water Res. 233, 119794.

Jiang, M., Hu, L., Lu, A., Liang, G., Lin, Z., Zhang, T., Xu, L., Li, B., Gong, W., 2020. Strong sorption of two fungicides onto biodegradable microplastics with emphasis on the negligible role of environmental factors. Environ. Pollut. 267, 115496.

Kadhom, M., Kalash, K., Al-Furaiji, M., 2022. Performance of 2D MXene as an adsorbent for malachite green removal. Chemosphere 290, 133256.

Kwon, B.G., Koizumi, K., Chung, S.-Y., Kodera, Y., Kim, J.-O., Saido, K., 2015. Global styrene oligomers monitoring as new chemical contamination from polystyrene plastic marine pollution. J. Hazard. Mater. 300, 359–367.

K.L. Law, R.C. Thompson, Oceans. Microplastics in the seas, Science (New York, N.Y.), 345 (2014) 144–145.

Leslie, H.A., van Velzen, M.J.M., Brandsma, S.H., Vethaak, A.D., Garcia-Vallejo, J.J., Lamoree, M.H., 2022. Discovery and quantification of plastic particle pollution in human blood. Environ. Int. 163, 107199.

Li, Y., Zhang, Y., Su, F., Wang, Y., Peng, L., Liu, D., 2022. Adsorption behaviour of microplastics on the heavy metal Cr(VI) before and after ageing. Chemosphere 302, 134865.

Liu, P., Zhan, X., Wu, X., Li, J., Wang, H., Gao, S., 2020a. Effect of weathering on environmental behavior of microplastics: properties, sorption and potential risks. Chemosphere 242, 125193.

Liu, P., Lu, K., Li, J., Wu, X., Qian, L., Wang, M., Gao, S., 2020b. Effect of aging on adsorption behavior of polystyrene microplastics for pharmaceuticals: Adsorption mechanism and role of aging intermediates. J. Hazard. Mater. 384, 121193.

Liu, X., Sun, P., Qu, G., Jing, J., Zhang, T., Shi, H., Zhao, Y., 2021. Insight into the characteristics and sorption behaviors of aged polystyrene microplastics through three type of accelerated oxidation processes. J. Hazard. Mater. 407, 124836.

Lv, W., Zhou, W., Lu, S., Huang, W., Yuan, Q., Tian, M., Lv, W., He, D., 2019. Microplastic pollution in rice-fish co-culture system: A report of three farmland stations in Shanghai, China. Sci. Total Environ. 652, 1209–1218.

Mao, R., Lang, M., Yu, X., Wu, R., Yang, X., Guo, X., 2020. Aging mechanism of microplastics with UV irradiation and its effects on the adsorption of heavy metals. J. Hazard. Mater. 393, 122515.

Masiá, P., Ardura, A., Garcia-Vazquez, E., 2019. Microplastics in special protected areas for migratory birds in the Bay of Biscay. Mar. Pollut. Bull. 146, 993–1001.

Miao, F., Liu, Y., Gao, M., Yu, X., Xiao, P., Wang, M., Wang, S., Wang, X., 2020. Degradation of polyvinyl chloride microplastics via an electro-Fenton-like system with a TiO2/graphite cathode. J. Hazard. Mater. 399, 123023.

Mu, J., Qu, L., Jin, F., Zhang, S., Fang, C., Ma, X., Zhang, W., Huo, C., Cong, Y., Wang, J., 2019. Abundance and distribution of microplastics in the surface sediments from the northern Bering and Chukchi Seas. Environ. Pollut. 245, 122–130.

Napper, I.E., Davies, B.F.R., Clifford, H., Elvin, S., Koldewey, H.J., Mayewski, P.A., Miner, K.R., Potocki, M., Elmore, A.C., Gajurel, A.P., Thompson, R.C., 2020. Reaching new heights in plastic pollution—preliminary findings of microplastics on Mount Everest. One Earth. 3, 621–630.

Neves, D., Sobral, P., Ferreira, J.L., Pereira, T., 2015. Ingestion of microplastics by commercial fish off the Portuguese coast. Mar. Pollut. Bull. 101, 119–126.

Peeken, I., Primpke, S., Beyer, B., Gütermann, J., Katlein, C., Krumpen, T., Bergmann, M., Hehemann, L., Gerdts, G., 2018. Arctic sea ice is an important temporal sink and means of transport for microplastic. Nat. Commun. 9, 1505.

Peng, X., Chen, M., Chen, S., Dasgupta, S., Bai, S., 2018. Microplastics contaminate the deepest part of the world's ocean. Geochem Perspect. Lett. 9, 1–5.
Potthoff, A., Oelschlägel, K., Schmitt-Jansen, M., Rummel, C.D., Kühnel, D., 2017. From the sea to the laboratory: characterization of microplastic as prerequisite for the assessment of ecotoxicological impact. Integr. Environ. Assess. Manag. 13, 500–504.
Prokić, M.D., Radovanović, T.B., Gavrić, J.P., Faggio, C., 2019. Ecotoxicological effects of microplastics: examination of biomarkers, current state and future perspectives. TrAC, Trends Anal. Chem. 111, 37–46.
Rivaton, A., Gardette, J.L., 1998. Photooxidation of aromatic polymers. Angew. Makromol. Chem. 261, 173–188.
Romera-Castillo, C., Pinto, M., Langer, T.M., Álvarez-Salgado, X.A., Herndl, G.J., 2018. Dissolved organic carbon leaching from plastics stimulates microbial activity in the ocean. Nat. Commun. 9, 1430.
Singh, B., Sharma, N., 2008. Mechanistic implications of plastic degradation. Polym. Degrad. Stab. 93, 561–584.
de Souza Machado, A.A., Kloas, W., Zarfl, C., Hempel, S., Rillig, M.C., 2018. Microplastics as an emerging threat to terrestrial ecosystems. Glob. Change Biol. 24, 1405–1416.
Su, L., Xue, Y., Li, L., Yang, D., Kolandhasamy, P., Li, D., Shi, H., 2016. Microplastics in Taihu Lake, China. Environ. Pollut. 216, 711–719.
Suhrhoff, T.J., Scholz-Böttcher, B.M., 2016. Qualitative impact of salinity, UV radiation and turbulence on leaching of organic plastic additives from four common plastics — a lab experiment. Mar. Pollut. Bull. 102, 84–94.
Sun, Y., Yuan, J., Zhou, T., Zhao, Y., Yu, F., Ma, J., 2020. Laboratory simulation of microplastics weathering and its adsorption behaviors in an aqueous environment: a systematic review. Environ. Pollut. 265, 114864.
Tewari, K., Singhal, G., Arya, R.K., 2018. Adsorption removal of malachite green dye from aqueous solution. Rev. Chem. Eng. 34, 427–453.
Wang, C., Xian, Z., Jin, X., Liang, S., Chen, Z., Pan, B., Wu, B., Ok, Y.S., Gu, C., 2020b. Photo-aging of polyvinyl chloride microplastic in the presence of natural organic acids. Water Res. 183, 116082.
Wang, K., Wang, K., Chen, Y., Liang, S., Guo, C., Wang, W., Wang, J., 2023a. Adsorption–desorption behavior of malachite green by potassium permanganate pre-oxidation polyvinyl chloride microplastics. Environ. Technol. Innov. 30, 103138.
Wang, K., Wang, K., Chen, Y., Liang, S., Zhang, Y., Guo, C., Wang, W., Wang, J., 2023b. Desorption of sulfamethoxazole from polyamide 6 microplastics: environmental factors, simulated gastrointestinal fluids, and desorption mechanisms. Ecotoxicol. Environ. Saf. 264, 115400.
Wang, T., Wang, L., Chen, Q., Kalogerakis, N., Ji, R., Ma, Y., 2020a. Interactions between microplastics and organic pollutants: effects on toxicity, bioaccumulation, degradation, and transport. Sci. Total Environ. 748, 142427.
Wang, X., Zheng, H., Zhao, J., Luo, X., Wang, Z., Xing, B., 2020a. Photodegradation elevated the toxicity of polystyrene microplastics to grouper (Epinephelus moara) through disrupting hepatic lipid homeostasis. Environ. Sci. Technol. 54, 6202–6212.
Wardrop, P., Shimeta, J., Nugegoda, D., Morrison, P.D., Miranda, A., Tang, M., Clarke, B.O., 2016. Chemical pollutants sorbed to ingested microbeads from personal care products accumulate in fish. Environ. Sci. Technol. 50, 4037–4044.
Wei, W., Huang, Q.-S., Sun, J., Wang, J.-Y., Wu, S.-L., Ni, B.-J., 2019. Polyvinyl chloride microplastics affect methane production from the anaerobic digestion of waste activated sludge through leaching toxic bisphenol-A. Environ. Sci. Technol. 53, 2509–2517.
Xu, B., Liu, F., Brookes, P.C., Xu, J., 2018. The sorption kinetics and isotherms of sulfamethoxazole with polyethylene microplastics. Mar. Pollut. Bull. 131, 191–196.
Yu, F., Yang, C., Huang, G., Zhou, T., Zhao, Y., Ma, J., 2020. Interfacial interaction between diverse microplastics and tetracycline by adsorption in an aqueous solution. Sci. Total Environ. 721, 137729.
Zantis, L.J., Carroll, E.L., Nelms, S.E., Bosker, T., 2021. Marine mammals and microplastics: a systematic review and call for standardisation. Environ. Pollut. 269, 116142.
Zhu, J., Yu, X., Zhang, Q., Li, Y., Tan, S., Li, D., Yang, Z., Wang, J., 2019. Cetaceans and microplastics: First report of microplastic ingestion by a coastal delphinid, Sousa chinensis. Sci. Total Environ. 659, 649–654.